

# Effects of Radiation and SAR from Wireless Implanted Medical Devices on the Human Body

Pichitpong Soontornpipit PhD\*

\* Department of Biostatistics, Faculty of Public Health, Mahidol University, Bangkok, Thailand

**Objective:** To study the effect and impact from electromagnetic field radiation and specific absorption rate (SAR) on the human body.

**Material and Method:** The present study describes a quasi-experimental research. The implanted antenna embedded to the medical device such as the cardiac pacemaker was designed in the human phantom using finite-difference time-domain method. The skin mimicking gels were developed as the tissue stimulant to realistically represent the human body.

**Results:** The dual-band implantable antenna is designed to operate at 400 MHz and 2.4 GHz and is used to determine the level of electromagnetic field radiated and SAR levels from implanted biosensors. The SAR limitations, maximum gain, maximum temperature rise in the body model and the radiation efficiency on each operating frequency are determined to provide the safety level.

**Conclusion:** The research results indicate that SAR and safety limitations are body and frequency dependent. High-performance and low-operated power dual-band PIFA antenna for development of the next generation of medical implants operating on the MICS and the ISM bands will facilitate clinically significant improvements in healthcare.

**Keywords:** Biotelemetry, Implantable antenna, Medical device, Specific absorption rate (SAR)

*J Med Assoc Thai* 2012; 95 (Suppl. 9): S189-S197

Full text. e-Journal: <http://jmat.mat.or.th>

Biotelemetry is the process of conveying information from devices inside human body to another in the absence of hard-wired cable links<sup>(1)</sup>. With biotelemetry, patient can be monitored under normal conditions and in natural surroundings. Since the first successful use of biotelemetry devices to transmit and receive the information, biotelemetry has become one of the most widely accepted and evolving disciplines used in many other medical applications. These medical implants include cardiac ablation, implantable drug pumps, cochlea implants, artificial eyes, muscle stimulators, balloon angioplasty and cancer treatment using hyperthermia<sup>(2-5)</sup>. Monitored parameters generally include temperature, muscle movement and motion, pH, blood pressure and other bio-potential data. Biotelemetry provides numerous advantages over conventional methods including continuous physiological monitoring, avoiding a single intrusive event that may disrupt normal routine. Its continued progress has resulted from advances in technology that have allowed transmitters to become smaller and lighter with sensor peripherals for measuring numerous

environmental parameters<sup>(6,7)</sup>. While much has been done in the applications of communication technology and methods for biotelemetry, there are few examples for implantable medical devices. This is due to the concern on safety of radiation power from the wireless unit in medical devices.

Electromagnetic field from implantable biosensors damages the surrounding implanted environments if exposed too long. The goal of short-term sensing of pH and pressure in blood, tissue and body fluids can be achieved without the dramatically negative radiation effect. However, the stable sensors and monitors for long-term implantation such as cardiac pacemaker continue to elude researchers<sup>(8-11)</sup>. Thus long-term sensing and monitoring data are critical for implant biocompatibilities regarding to their safety to the human body and its surrounding tissues. In order to minimize the radiation effect from electromagnetic field, the degree of power handling must be limited. The European Telecommunications Standards Institute (ETSI) has standardized two additional frequency bands that are available for this medical application. The first band operates at 402-405 MHz as the Medical Implant Communication System (MICS). This frequency band has the benefit of being reserved mainly for medical and metrological applications. The 2.4-2.5 GHz industrial, scientific and medical (ISM) band

**Correspondence to:**

Soontornpipit P, Department of Biostatistics, Faculty of Public Health, Mahidol University, Bangkok 10400, Thailand.

Phone: 0-2245-8530, 0-2245-8542

E-mail: [soontornpipit@gmail.com](mailto:soontornpipit@gmail.com)

is chosen as the second operating frequency. The ISM band has an advantage over the MICS band from having lower loss when penetrated through the body, but has the drawback of being heavily used by other applications such as wireless computer networks, medical diathermy machines and microwave ovens. The medical devices that use the 2.45 GHz frequency band can generate a strong electromagnetic interference and therefore disrupt the communication link if the same operating frequency is used for a full-duplex. The ETSI document also lists two more principal fields for the safety standard. The first one is for communication between a base station and an implanted device. The second one is for communication between medical implants within the same body. The results from these documents are evaluated in terms of their impact on the link budget from the prototypes of MICS and ISM systems. Conclusions on the necessary complexity of the transceivers and transponders are analyzed to fully exploit the potential of the communication link. SAR levels of the communication unit in implanted devices have to be at a safe level to avoid damage to neighboring radio services and human bodies. The Federal Communications Commission (FCC) guidelines differentiate between portable and mobile devices according to their proximity to exposed persons. Human exposure to radio frequency (RF) emissions from mobile devices can be evaluated with respect to Maximum Permissible Exposure (MPE) limits for field strength or power density or with respect to SAR limits.

SAR is considered as an index that quantifies the rate of energy absorption in biological tissues. It is an important parameter when designing the overall implantable medical devices with attentions. SAR can be evaluated using simulated tissue medium contained in a realistic human shaped phantom shell. This method allows a miniature electric field probe to measure the electric field within the tissue regions exposed to the transmitter configured in normal operating positions. The characteristics of RF energy absorbed on human tissues are frequency dependent. The dielectric properties of simulated tissue media used for SAR evaluations must match the target tissue properties specified at the operating frequency range of the device. To determine the energy absorption in biological tissues, the limitation for the maximum effective radiated power (ERP) and the radiation efficiency of the device in the body must be utilized. The ERP is the product of the power delivered by the transmitted antenna and its gain. If a transmitter operates next to the body or at close proximity to persons, a RF evaluation may be

requested<sup>(12)</sup>. These types of evaluations are typically limited to transmitters according to the FCC's Report and Order in ET Docket 96-8<sup>(13)</sup>. To maintain consistency for SAR measurement and computational methods, the homogeneous phantom models are recommended. To compute SAR on inhomogeneous models, the tissue dielectric parameters based on the 4-Cole-Cole equation may be used<sup>(13)</sup>.

Many researches have been carried out to study the effects of RF radiation on human body using various exposure scenarios and models<sup>(14-18)</sup>. The interaction of radio waves with biological tissues from internal electromagnetic fields can be determined from Maxwell's equations with given boundary conditions. Calculating a RF link budget to determine the minimum and maximum handling powers would give similar advantages as it does to the wireless communication system. However, most of these studies have been focused on radiation effects from mobile phones and base stations to the human body. Even though there are reports shown that more and frequent communication and management of an implanted unit significantly increase the long-term complications of body tissues exposed to electromagnetic radiation. While considering the impressive progress in the use of implantable devices, there are risks regarding to the safety issues, electromagnetic compatibility and interferences from the devices. One of the most serious problems regarding the safety of biomedical devices is the potential for tissue heating. Little work has been done on the studies of radiation effects and radiation efficiency of wireless medical devices in interaction with body tissues. Few reports showed the radiation efficiency and radiation effects on wearable medical sensor devices. Therefore there are current needs to study the effects of implanted medical devices with embedded antennas, which are expected to play a dominant role in next-generation biotelemetry technologies since more and more implantable devices become clinically employed, such as cardiac ablation, implantable drug pumps, cochlea implants, and artificial eyes.

Usually an implantable device operating on low frequency has less biological effects than higher frequency due to less tissue absorption. However, with low carrier frequency, the embedded antenna needs to be physically small compared to the electrical wavelength. Medical devices that require embedding must be compact. While the implantable medical device with a low operating frequency has a limitation on the embedded antenna dimension, designing implantable

medical devices to operate on a high frequency needs to be characterized carefully so that the safety guidelines can be met. RF telemetry concepts on safety regulations have been developed to validate their effects and results in the presence of tissue-like phantoms<sup>(19-21)</sup>. The effects of multiple layers and different tissues in homogeneity and inhomogeneity have been analyzed but, with the dispersive properties of inhomogeneous tissues, the results are slightly improved on the uniformity of the radiation from embedded wireless unit. The effects of layered biological tissues on a biotelemetry link have been studied. For examples, the potential of SAR in human head exposed with the frequency bandwidth ranging from 10 MHz to 3 GHz by using the finite-difference time-domain (FDTD) method is demonstrated. Martinez-Burdalo analyzed SAR depositions in different-aged human heads. Their researches showed that biological effects of an embedded wireless device are also related to its position and orientation. Kim found that the radiated power was the largest when a dipole antenna was located at the center of head model in comparison with other positions<sup>(21)</sup>. However, they did not analyze the worst radiation intensity of human body model because of variation in the characteristic performance, orientation, and position dependent.

### **Material and Method**

The author designed the dual-band planar inverted F antenna (PIFA) operating at 402-405 MHz MICS band and 2.40-2.45 GHz ISM band and compared the electromagnetic effect when placed inside different locations of the human body. The device emulates biotelemetry application to communicate to the cardiac pacemaker, which is one of the common active medical implants. The pacemaker has a need for embedded antenna to transmit a new parameter set and receive measurements and statistics from it. Resonant characteristics of the implanted antennas and their radiation performances are studied. The radiated power and SAR from the antennas affected by the patient's size, body shape and position are presented to provide useful background information for hyperthermia and biotelemetry. Electromagnetic (EM) characteristics of the antenna implanted in a phantom human body are analyzed using the finite difference time domain method.

### **Results**

#### ***The link budget***

The International Telecommunication Union

has discussed the interference issues between MICS and the Meteorological Aids Systems (Metasids) in the document ITU-R SA.1346<sup>(22)</sup>. It includes a link budget calculated for uplink and downlink systems. The purpose of the calculations is to show that these MICS and ISM systems work properly and safely to minimize the risk of being disturbed by harmful interference. The MICS radio channel at 400 MHz differs from the traditional mobile-phone channels and ISM band. The system is intended for indoors with both the patient and the base station in the same room, while the ISM system is designed for both indoor and outdoor uses. On the other hand, the combination of the MICS band and the limited range makes the full potential use of the link budget on both possible and practical for the MICS band. The system link budget consists of two main parts: the communication from transmitter to the body and from the body to the antenna device. All parameters related to the thermal noise and losses from the links, fading, and multipath are well standardized. Reflections against the ceiling, walls, floor and other environments provide both additional noise and gain for different wave patterns. The gain of the implanted antenna varies in different directions assuming the highest gain is in a direction toward the implanted device. Also variations between different patients and consultations provide different gain and path losses. The variations of the path loss constitute different types of fading when they occur over time, as is the case with patient movement. Because the transmitting antenna can be placed both in vertical and horizontal polarization regarding to the patient orientation, the receiving antenna has to move to both co-polarization and cross-polarization in order to avoid the polarization loss.

In addition, the available power from the battery and the performance of the embedded antenna must be considered. For safety, the maximum EIRP must be limited to the power set in each standard. The standard of telemetry system for the implanted antenna has margins of 17.5 and 16.8 dB to the MICS and ISM, respectively. These margins are set in order to conserve the battery power in the implant unit. The path loss is taken as free space loss and only valid for a transmitter and a receiver in the far field conditions. An additional factor, representing excess losses, is also added. It includes patient orientation, antenna misalignment, non-line of sight conditions and polarization loss. The loss factors have been thoroughly investigated in the document. One of the critical parameters in the ITU-R link budget is the gain characteristic of the implanted antenna. While the noise and loss levels are usually

based on the communication method and the amount of energy available from the radiated power, the antenna performance relies heavily on the movement of the patient and other orientations aspects. Thus the design criteria such as operating environment must be focused. An overview of the link budget from ITU-R is given in Table 1.

### ***Developments of tissue mimicking gels***

In order to verify performance of an implanted antenna in the body, the research makes use of tissue simulating liquids. Characterizations of tissue-mimicking materials are necessary for implantable systems as those used for measurement of the specific absorption rate (SAR) in evaluation of mobile handsets. Testing of systems in humans is not practical in development work because there are ethical restrictions, especially for technical testing and development of small subsystems<sup>(22)</sup>. The human body model is constructed from visible human body data and the dielectric properties of human biological tissues are referred to the results proposed by Gabriel<sup>(23)</sup>. For accurate analysis in interaction with human body, the heterogeneous human body meshes derived from the University of Utah man model<sup>(24)</sup> have 31 different tissues. It resembles the chest and the upper part of a human body with some constant curvatures, in contrast to the human who is mostly flat on the front and back sides. The entire body mesh consists of 380 x 186 x 190 cells where each cell contains the information of density, conductivity and relative permittivity associated with two different frequencies.

The dielectric permittivity, conductivities and mass density of tissues are shown in Table 2. The benefit of this procedure is that phantoms of different body positions and shapes can easily be generated, and that the process is repeatable. The phantom models do not represent any mean or median human shape for man or woman due to the original intention for marketing purposes and thus idealized versions of human shapes. Although FDTD is able to model the accurate body structures, there are still significant difficulties in modeling FDTD schemes such as graded mesh, sub-gridding, or an antenna model. The mesh size from the 400 MHz band would be too large for the 2.4 GHz band and would yield significantly different amounts of SAR. The differences of the SARs were proportionally related to the different volumes and the cell sizes. The cell size in this work was selected carefully in order to provide the radiation characteristics and 1-g averaged SAR distributions accurately. The mesh

size of the human body model is 2 x 2 x 2 mm<sup>3</sup> and the mesh cell size of the area around the implanted antenna is 1 x 1 x 2 mm<sup>3</sup> for 400 MHz MICS band. The volume of the body mesh at the cell size is 1 x 1 x 1 mm<sup>3</sup> for ISM band. These mesh sizes are considered large if most energy is absorbed in this area. Increasing human body mesh for the less radiated parts is acceptable. The cell size of 1 mm<sup>3</sup> is still acceptable even at the frequency of 2.4 GHz. The 3-D geometry of the FDTD simulations for the antenna design is given in Fig. 1 and the structure of an implantable antenna is shown in Fig. 2.

### ***Development of the Embedded PIFA Antennas***

The gel tissues that mimicked the electrical properties of the human body were developed and used to test the performance of the antenna prototype. The gels consist of de-ionized water, sugar, salt and a TX-151 powder. The TX-151 powder is an inert substance that absorbs water and increases the viscosity of the solution. These mimicking gels were formed by adding a TX-151 powder in the liquid solution and gradually heating the solution until it mixed. The mixture is left in a room temperature to cool down. Dielectric constant and conductivity measurements are performed using Agilent's 85070E dielectric probe kit and an HP8510C network analyzer. Following these initial tests, recipes for simulant gels using for the MICS and ISM bands are carefully formulated. The measured properties of the human skin are taken from the literature<sup>(25,26)</sup>. Different recipes are given for each band because it is not possible to produce a valid approximation to human skin for the entire spectrum from 300 MHz to 3 GHz using a single formula. Due to that, some shifts in frequency caused by the difference in electrical properties of the TX-151 were indeed observed. The electrical constants and conductivities of the skin at 402 MHz were 48.94 and 0.71 S/m and at 2.4 GHz were 39.72 and 1.48 S/m, respectively. Table 3 shows the concentrations of ingredients in both gels.

A typical cardiac pacemaker has a dimension of 30 x 26 x 10 mm<sup>3</sup> as shown in Fig. 3, but the demand requires continually smaller designs. Miniaturized antennas are needed in the near future, consequently the PIFA antenna was designed and performances such as the operating frequency and the return loss were tuned to meet the requirements. The antenna has a cell size of 1 x 1 x 1 mm. The biocompatible substrate material is Rogers RO3210 ( $\epsilon_r = 10.2$ ,  $\delta = 0.003$ ). The superstrate is silicone ( $\epsilon_r = 7.1$ ,  $\delta = 0.002$ ), used to insulate the implanted antenna from shorting out in the body and to decrease the effects of highly conductive

**Table 1.** The link budget from ITU-R document

Uplink from implant	ITU-R for MICS	ITU-R for ISM
BW	200 kHz	98 MHz
TX Power	15.5 dBm	12.8 dBm
Antenna Gain	-31.5 dBi	-35.5 dBi
EIRP	-16 dBm	- 19 dBm
Free Space Loss (2m)	30.5 dB	37 dB
Fade Margin	10 dB	12.5 dB
Excess Loss	15 dB	18 dB
Base station gain	2 dBi	3 dBi
Receiver noise at input	-101 dBm	-106 dBm
Received power at base	-69.5 dBm	-65.5 dBm
Path Loss	-72 dBm	-78 dB
Downlink to implant	ITU-R for MICS	ITU-R for ISM
BW	30 kHz	17 MHz
TX Power	18 dBm	20 dBm
Antenna Gain	2 dBi	4.5 dBi
EIRP	-16 dBm	-21 dBm
Free Space Loss (2m)	30.5 dB	37 dB
Fade Margin	10 dB	12.5 dB
Excess Loss	15 dB	18 dB
Body antenna gain	-30.5 dBi	-36 dB
Received power in body	-102 dBm	-107 dBm
Receiver noise at input	-121 dBm	-126 dBm
Path Loss	-84 dBm	-89 dBm

**Table 2.** Dielectric constant, conductivities and mass density for biological tissues of the simulation

Tissue	$\epsilon_r$	$\sigma_c$ (S/m)	Mass Density ( $10^3$ kg/m <sup>3</sup> )
Fat	11.60	0.08	0.92
Skin	46.68	0.64	1.01
Skin (dry)	46.70	0.69	1.01
Skin (wet)	49.80	0.67	1.01
Muscle	57.10	0.79	1.04
2/3-Muscle	42.07	0.64	1.04
Bone	22.40	0.23	1.06
Blood	57.29	1.72	1.06
Cartilage	43.64	0.65	1.10
Lung	21.58	0.35	1.01
Heart	66.0	0.97	1.05
Liver	51.20	0.65	1.05
Kidney	66.40	1.10	1.05
Cerebro Spinal	71.20	2.25	1.01
Spinal Core	35.40	0.45	1.04
Bone marrow	5.67	0.03	1.06
Trachea	44.20	0.64	1.10
Stomach	67.50	1.00	1.05
Colon	66.10	1.90	1.05
Spleen	63.20	1.03	1.05z

biological tissue. It protects the organs and human tissues surrounding the implanted antenna by reducing

RF power at the locations of lossy human tissues. The implanted antenna was simulated to match with a 50-

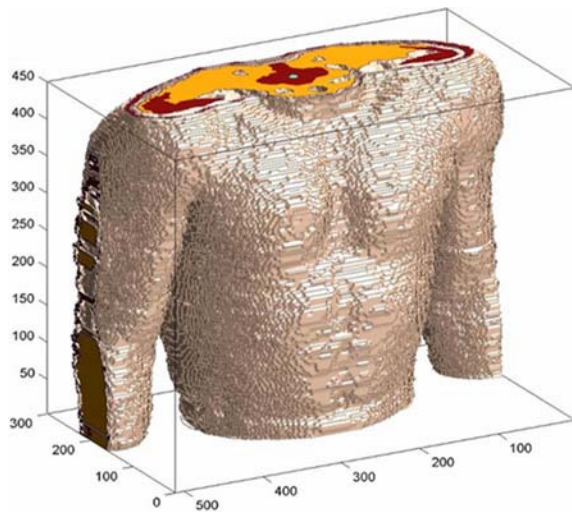


**Fig. 1** Three-dimensional FDTD human body used for the implanted antenna

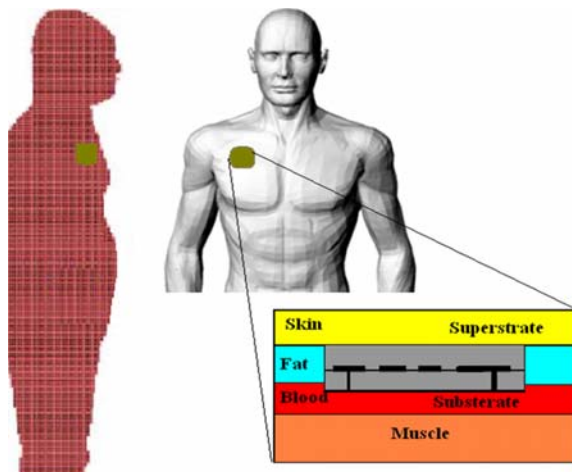


**Fig. 2** Structure of an implantable antenna



**Fig. 3** Cardiac pacemaker

**Table 3.** Recipes for mimicking tissues for MICS and ISM bands

Tissue	MICS band	ISM band
Salt	3.2%	2.3%
Sugar	50.6%	48.2%
Water	46.2%	49.5%
TX-151 powder	1 g/100 ml	1 g/100 ml

ohm load resistor in order to reduce or eliminate the reflection, and thus lower the radiated heat. The values of the terminating impedance at 400 MHz and 2.4 GHz when implanted changed as the contact point is encapsulated by the body in the chronic implantation phase. The implanted location is put closer to the outer layer of the phantom model for the less power attenuation and absorption. The implanted location in the phantom model has a sizeable effect on the communication performance. The software XFDTD from Remcom<sup>(27)</sup> is used to analyze SAR and antenna performances.

SAR and the temperature rise value were normalized to the 1 mW input power. The accuracies of the antenna simulation at 1 mm<sup>3</sup> resolution under the frequency of 400 MHz and 2.4 GHz were acceptable. The performances were compared in the simulation of the adaptive mesh (The cell size in the area of the antenna is 1 x 1 x 1 mm, while the mesh cell size in the other area is 2 x 2 x 3 mm) of XFDTD software and found that it provided similar results. The dimension of the PIFA is shown in Fig. 4. The coaxial feed is located for a good 50-ohm match. Simulated and measured resonant characteristics related to the spiral PIFA are compared in Fig. 5. The good agreement between simulation and measurement results indicates that the antenna is substitutable for the complex human body.

The variations of SAR and gain from different positions were evaluated with the FDTD method in XFDTD. The locations of the PIFA antenna were adjusted to three different positions in order to get an estimate of the variations and the radiating fields. The antenna was measured through the vertical axis of the human phantom. It represented the implanted antenna location, but sometimes this position failed to keep the antenna constant between different postures and different phantoms. The resulting gain reductions, SAR and other parameters from the coverage are shown in Table 5. Table 6 presents the maximum gain and radiation efficiency of three body sizes: normal, thin, and fat. The thin- and fat- man phantoms varied  $\pm 20\%$

around the mass index. It shows a strong dependence on the phantom shape.

**Potential conflicts of interest**

None.

**References**

1. IEEE Standard for safety levels with respect to

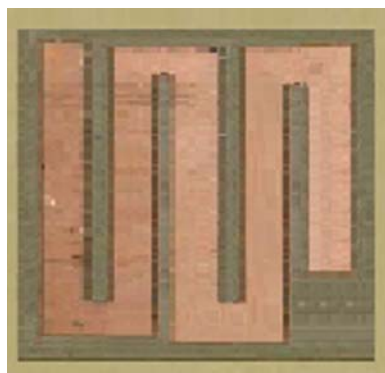


**Fig. 4** The spiral PIFA antennas designed for the implantable device in the human chest

human exposure to radio frequency electromagnetic fields, 3 KHz to 300 GHz. New York: The Institute of Electrical and Electronics Engineers; 1999.

2. IEEE Recommended practice for determining the peak spatial-average specific absorption rate (SAR) in the human head from wireless communications

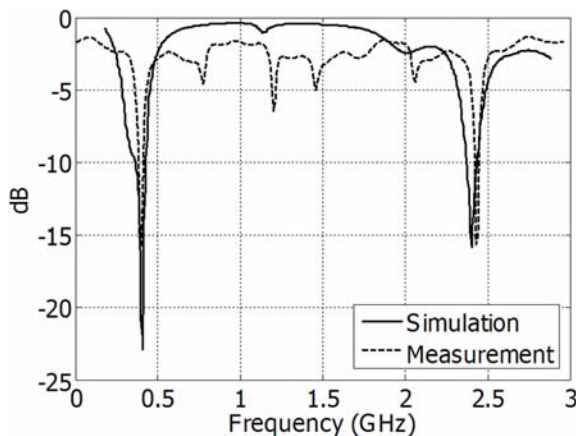


**Fig. 5** The simulation and measurement results

**Table 4.** Reduction of the gain for a given percentage of the body coverage

Plane	400MHz Coverage Area		2.4 GHz Coverage Area	
	90%	95%	90%	95%
Transversal	3.84 dB	3.95 dB	4.43 dB	4.56 dB
Straight	7.56 dB	9.97 dB	10.80 dB	13.40 dB
Entry	5.83 dB	7.12 dB	8.35 dB	9.11 dB

**Table 5.** The SAR peak, maximums of SAR 10g and SAR 1g, maximum gain, maximum temperature rise in the body model, and radiation efficiency at delivered power of 1 mW

Frequency	SAR peak	SAR 10g	SAR 1g	G <sub>Max</sub>	Temp <sub>rise</sub>	Rad Eff
400 MHz	28.7	0.54	2.91	-28 dB	0.25°C	1.8%
2.4 GHz	6.13	0.28	0.92	-21 dB	0.14°C	7.4%

**Table 6.** Maximum gain and radiation efficiency for different body sizes

Phantom Shape	400 MHz		2.4 GHz	
	G <sub>Max</sub>	Red Eff	G <sub>Max</sub>	Red Eff
Normal-Man	-28 dB	1.8%	-21 dB	7.4%
Thin-Man	-26.7 dB	2.2%	-18.4 dB	12.9%
Fat-Man	-29.6 dB	1.1%	-22.5 dB	5.6%

- devices: measurement techniques IEEE: New York: The Institute of Electrical and Electronics Engineers; 2003.
3. Gandhi OP, Kang G. Some present problems and a proposed experimental phantom for SAR compliance testing of cellular telephones at 835 and 1900 MHz. *Phys Med Biol* 2002; 47: 1501-18.
  4. Dimbylow PJ. Fine resolution calculations of SAR in the human body for frequencies up to 3 GHz. *Phys Med Biol* 2002; 47: 2835-46.
  5. Martinez-Burdalo M, Martin A, Anguiano M, Villar R. Comparison of FDTD-calculated specific absorption rate in adults and children when using a mobile phone at 900 and 1800 MHz. *Phys Med Biol* 2004; 49: 345-54.
  6. Alomainy A, Hao Y, Parini CG, Hall PS. Comparison between two different antennas for UWB on-body propagation measurement. *Antennas Wireless Propag Lett* 2005; 4: 31-4.
  7. Yang GZ. *Body sensor networks*. London: Springer; 2006.
  8. Budinger TF. Biomonitoring with wireless communications. *Annu Rev Biomed Eng* 2003; 5: 383-412.
  9. Schuster JW, Luebbers RJ. An FDTD algorithm for transient propagation in biological tissue with a Cole-Cole dispersion relation. Atlanta, GA: IEEE AP/URSI; 1998.
  10. Steinhaus BM, Smith RE, Crosby P. The role of telecommunications in future implantable device systems. In: *Proceedings of the 16th Annual International Conference of the IEEE*; 3-6 Nov, 1994; Baltimore, MD, USA.
  11. Durney CH, Iskander MF. *Antenna handbook in antennas for medical applications*. New York: Van Nostrand; 1988.
  12. Rosen A, Stuchly MA, Vorst AV. Applications of RF/microwaves in medicine. *IEEE Trans Microwave Theory Tech* 2002; 50: 963-74.
  13. The Federal Communications Commission. Regulation [Internet]. 2012 [cited 2012 Mar 15]. Available from: <http://www.fcc.gov>.
  14. American National Standards Institute. 2012 [cited 2012 Mar 15]. Available from: <http://www.ansi.org>.
  15. Soontornpipit P. Design of implantable antennas for communication with medical implants [thesis]. Logan: Utah State University; 2002.
  16. Soontornpipit P, Furse CM, Chung YC. Design of implantable microstrip antennas for communication with medical implants. *Microwave Theory and Techniques, IEEE Transactions Antennas and Propagation, IEEE Transactions* 2004; 52: 1944-51.
  17. Bylapudi RD. Analysis of helical antennas imbedded in lossy dielectric material [thesis]. Logan: Utah State University; 2002.
  18. Wessels D. Implantable pacemakers and defibrillators: device overview and EMI considerations. *Electromagnetic Compatibility, 2002. EMC 2002. IEEE International Symposium*. 19-23 Aug, 2002; Minneapolis, MN, USA. 2002: 911-5.
  19. Scanlon WG, Evans NE, McCreesh ZM. RF performance of a 418 MHz radio telemeter packaged for human vaginal placement. *IEEE Trans Biomed Eng* 1997; 44: 427-30.
  20. Scanlon WG, Evans NE, Burns JB. FDTD analysis of closecoupled 418 MHz radiating devices for human biotelemetry. *Phys Med Biol* 1999; 44: 335-45.
  21. Kim J, Rahmat-Samii Y. An implantable antenna in the spherical human head: SAR and communication link performance. *Wireless Communication Technology, 2003. IEEE Topical Conference*. 15-17 Oct, 2003: 202-3.
  22. Medical Implant Communications Service (MICS) federal register. *Rules and Regulations* 1999; 64: 926-69,934.
  23. Gabriel S, Lau RW, Gabriel C. The dielectric properties of biological tissues: II. Measurements in the frequency range 10 Hz to 20 GHz. *Phys Med Biol* 1996; 41: 2251-69.
  24. Soontornpipit P, Furse CM, Chung YC. Miniaturized biocompatible microstrip antenna using a genetic algorithm. *Antennas and Propagation, IEEE Transactions* 2005; 53: 1939-45.
  25. Flamm D. Biocompatible materials for microstrip pacemaker antenna [senior project]: Logan: Utah State University; 2002.
  26. King RWP, Smith GS. *Antennas in matter: fundamentals, theory, and applications*. Cambridge, MA: The MIT Press; 1981.
  27. Remcom [Internet]. Finite Different Time Domain (FDTD): Tutorial. 2012 [cited 2012 Mar 15]. Available from: <http://www.remcom.com>

---

## ผลกระทบของการแพร่คลื่นและการดูดซึมจำเพาะของอุปกรณ์ทางการแพทย์ที่ถูกฝังในร่างกายของมนุษย์

พิจิตรพงศ์ สุนทรพิพิธ

**วัตถุประสงค์:** เพื่อศึกษาผลกระทบของคลื่นแม่เหล็กไฟฟ้าที่แพร่ออกมา รวมถึงอัตราการดูดซึมจำเพาะที่มีต่อร่างกายของมนุษย์

**วัสดุและวิธีการ:** การศึกษาครั้งนี้เป็นการศึกษาที่ทดลองเพื่อศึกษาสายอากาศที่ถูกฝังลงไปในร่างกายของมนุษย์พร้อมกับอุปกรณ์ทางการแพทย์ เช่น เครื่องกระตุ้นหัวใจในแบบโมเดลจำลองโดยใช้ทฤษฎี finite-difference time-domain (FDTD) และเจลจำลองที่มีคุณสมบัติคล้ายร่างกายของมนุษย์ได้ถูกพัฒนาเพื่อใช้ในการวัดผลกระทบ

**ผลการศึกษา:** สายอากาศสองความถี่ ทำงานที่ 400 เมกกะเฮิร์ตและ 2.4 กิกะเฮิร์ต ได้ถูกพัฒนาขึ้นมาเพื่อวัดผลกระทบของคลื่นแม่เหล็กไฟฟ้าที่มาจากอุปกรณ์ทางการแพทย์ที่ถูกฝังลงไปในร่างกาย ข้อจำกัดของ SAR กำลังขยายสูงสุดอุณหภูมิที่เพิ่มขึ้นในร่างกายและประสิทธิภาพการแผ่คลื่นสำหรับความถี่แต่ละความถี่ได้ถูกทดลองเพื่อให้ได้ระดับที่ปลอดภัย

**สรุป:** จากผลการศึกษาได้แสดงให้เห็นว่า ระดับของ SAR และข้อจำกัดต่างๆด้านความปลอดภัยขึ้นอยู่กับสภาพและขนาด ของร่างกายรวมทั้งย่านความถี่ที่ใช้งาน สายอากาศที่มีประสิทธิภาพสูง และใช้พลังงานน้อยได้ถูกออกแบบมาให้ทำงานที่ย่านความถี่ MICS และ ISM สามารถตอบสนองการพัฒนาทางด้านคลินิกของการดูแลสุขภาพเพื่อที่เป็นนวัตกรรมใหม่ๆ ของอุปกรณ์ทางการแพทย์ที่ถูกฝังในอนาคต

---